

Unusual electric polarization behavior in elemental quasi-two-dimensional allotropes of selenium

Dan Liu ^{1,*}, Lin Han,¹ Ran Wei ¹, Shixin Song,¹ Jie Guan,¹ Shuai Dong,¹ and David Tománek ^{2,†}¹*School of Physics, Southeast University, Nanjing, 211189, People's Republic of China*²*Physics and Astronomy Department, Michigan State University, East Lansing, Michigan 48824, USA*

(Received 23 May 2022; revised 31 August 2022; accepted 27 September 2022; published 14 October 2022)

We investigate tunable electric polarization and electronic structure of quasi-two-dimensional (quasi-2D) allotropes of selenium, which are formed from their constituent one-dimensional (1D) structures through an interchain interaction facilitated by the multivalence nature of Se. Our *ab initio* calculations reveal that different quasi-2D Se allotropes display different types of electric polarization, including ferroelectric (FE) polarization normal to the chain direction in α and δ allotropes, noncollinear ferrielectric (FiE) polarization along the chain axis in τ -Se, and anti-ferroelectric (AFE) polarization in η -Se. The magnitude and direction of the polarization can be changed by a previously unexplored rotation of the constituent chains. In that case, an in-plane polarization direction may change to out-of-plane in α -Se and δ -Se, flip its direction, and even disappear in τ -Se. Also, the band gap may be reduced and changed from indirect to direct by rotating the constituent chains about their axes in these quasi-2D Se allotropes.

DOI: [10.1103/PhysRevMaterials.6.103403](https://doi.org/10.1103/PhysRevMaterials.6.103403)

I. INTRODUCTION

It is not widely known that the term *ferroelectric* (FE) has been coined already in 1912 by Erwin Schrödinger as an electric counterpart to a ferromagnet [1]. At low enough temperatures, ferromagnetic or ferroelectric behavior is manifested by a permanent magnetic or electric polarization of a material that changes its direction upon applying an external field during a hysteretic process. Less than a decade after Schrödinger dismissed—immediately after proposing it—the concept of ferroelectricity as unrealistic, ferroelectric behavior was identified experimentally in Rochelle salt [2,3]. There is a long way from Rochelle salt to new, low-dimensional ferroelectrics that have captured the attention of the scientific community by their complex behavior and their potential application in electronics. This is particularly true for recently discovered 2D “van der Waals” (vdW) layered structures with ferroelectric behavior and different origins of polarization [4–8]. Best-known displacive ferroelectrics derive their behavior from a relative displacement of sublattices, which is characterized by the position of a representative atom within the unit cell. Changes in polarization, typically along a given direction, may be caused by applying an external electric field, such as in thin-film BaTiO₃ [9,10]. Only in specific 3D materials including PbTiO₃ [11], a strain gradient has been shown to modify the electrical polarization by an effect sometimes dubbed “flexoelectricity” [12]. Flip of the polarization direction has been observed in 2D vdW systems, such as ZrI₂, where shear strain has changed the symmetry of the system [13,14]. In these systems, whether due to an external electric field or mechanical strain, polarization changes have been limited to changes in the magnitude, whereas the polarization direction

remained the same or flipped by 180°. Capability to modify both magnitude and direction of polarization will open a whole new perspective for the application of 2D FE materials.

In this study, we investigate the polarization and band structure of four quasi-2D allotropes of Se, which we call α -Se, δ -Se, η -Se, and τ -Se. These quasi-2D allotropes are formed from their constituent one-dimensional (1D) compounds we call the *a*-helix, *b*-chain, *c*-helix, and *d*-chain, which possess a rotational degree of freedom about their axis. All atoms in the isolated 1D structures have two neighbors at the same distance and are structurally as well as electronically equivalent. In the quasi-2D allotropes, however, differences arise among individual atoms due to the interchain interaction. Our *ab initio* density functional theory (DFT) calculations reveal that the Bader charge of inequivalent Se sites deviates from six valence electrons, indicating the possibility of a macroscopic electric polarization.

As we will discuss further on, we find a FE polarization in α -Se and δ -Se, whereas η -Se behaves as an antiferroelectric (AFE). τ -Se behaves as a noncollinear ferrielectric (FiE), with FE polarization along the chain axis and AFE polarization in the out-of-plane direction. Rotating each constituent 1D chain of these quasi-2D Se allotropes changes the atomic symmetry, causing a change in the electrical properties. As for α -Se and δ -Se, the in-plane polarization can be changed to the out-of-plane direction. At specific rotation angles, τ -Se distorts to a highly symmetric structure and its FiE polarization disappears. Rotation of the constituent 1D chains in the quasi-2D allotropes also changes the band structure. We observe a modification of the fundamental band gap and a change from an indirect to a direct band gap in δ -Se.

II. COMPUTATIONAL TECHNIQUES

Our calculations of the stability, equilibrium structure, and energy changes during structural transformations have

*liudan2@seu.edu.cn

†tomanek@msu.edu

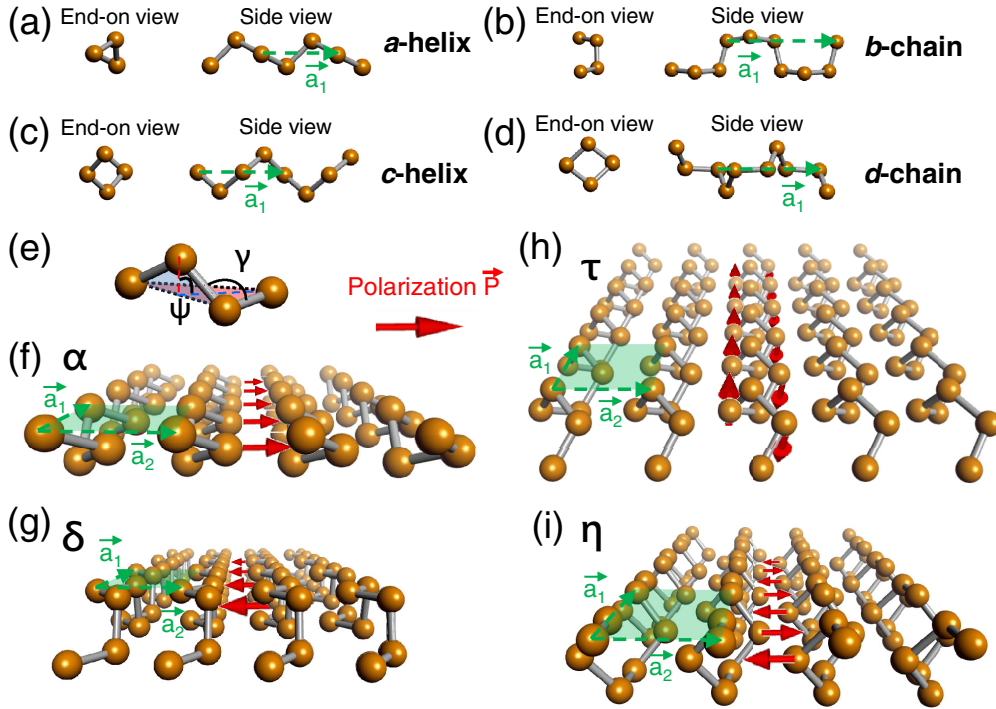


FIG. 1. Atomic structure of 1D allotropes of Se, namely (a) *a*-helix, (b) *b*-chain, (c) *c*-helix, and (d) *d*-chain. (e) Definition of the bond angle γ and the dihedral angle ψ used to characterize the structures. Also shown is the atomic structure of the corresponding quasi-2D allotropes (f) α -Se, (g) δ -Se, (h) τ -Se, and (i) η -Se. Red arrows indicate the local electric polarization. The unit cells of the quasi-2D structures are highlighted by the transparent green areas in (f), (g), (h), and (i).

been performed using the density functional theory (DFT) as implemented in the VASP [15,16] code. We used the Perdew-Burke-Ernzerhof (PBE) [17] exchange-correlation functional, augmented by the vdW correction using the DFT-D2 approach [18] to describe the interchain interaction. Periodic boundary conditions have been used throughout the study, with monolayers represented by a periodic array of slabs separated by a 30 Å thick vacuum region. The calculations were performed using the projector augmented wave (PAW) method [16] and 500 eV as energy cutoff. The reciprocal space has been sampled by a fine grid [19] of 9×11 k points in the 2D Brillouin zone (BZ) of α -Se, 8×8 k points in τ -Se, and 5×11 k points in the δ -Se and η -Se structures. All geometries have been optimized using the conjugate gradient (CG) method [20], until none of the residual Hellmann-Feynman forces exceeded 10^{-2} eV/Å. The polarization was calculated using the standard Berry phase approach [21,22] as implemented in the VASP code.

III. RESULTS

A. Atomic structure of quasi-2D Se allotropes and their electric polarization

One characteristic of group-VI elements is their propensity to form a variety of stable 1D structures including linear sulfur/selenium chains [23,24] and double-helices of selenium [25]. These structures can be characterized by bond angles γ and dihedral angles ψ , which are defined in Fig. 1(e). *a*-helices, shown in Fig. 1(a), consist of Se atoms connected to two neighbors with a bond angle $\gamma_a \approx 103^\circ$ and a dihedral angle $\psi_a \approx 100^\circ$, and can be found in bulk Se. Through an un-

twisting process, an *a*-helix can be transformed to a *c*-helix, as shown in Fig. 1(c), where $\gamma_c \approx 113^\circ$ and $\psi_c \approx 64^\circ$. By changing the dihedral angle, the *a*-helix can be transformed to a *b*- or a *d*-chain [24], as shown in Figs. 1(b) and 1(d). Two thirds of the bond angles in the *b*- and *d*-chains are found at $\gamma \approx 106^\circ$, the remaining one third at $\gamma \approx 103^\circ$. In the *b*-chain, one third of the dihedral angles is found at $\psi \approx 100^\circ$, and rest at $\psi \approx 90^\circ$, whereas in the *d*-chain, one third of the dihedral angles is at $\psi \approx 79^\circ$, and the rest at $\psi \approx 100^\circ$. Values close to the optimum bond angle $\gamma_{\text{opt}} \approx 106^\circ$ and the dihedral angle $\psi_{\text{opt}} \approx 83^\circ$, found earlier in unconstrained finite-length Se chains [24], explain the higher stability of the *b*- and *d*-chains in comparison to the *a*- and *c*-helices by about 17 meV/atom.

Facilitated by the multivalence nature of Se [26], these 1D Se structures can interact among each other, resulting in the formation of quasi-2D allotropes. In parallel to the parent 1D precursor *a*-helix, *b*-chain, *c*-helix, and *d*-chain, we call these quasi-2D allotropes α -Se, δ -Se [24], τ -Se, and η -Se [24]. Their unit cells are rectangular, with the Bravais lattice vector \vec{a}_1 directed along the chain axis and \vec{a}_2 in the interchain direction, and are shown in Figs. 1(f)–1(i). The bulk Se structure may be viewed as an assembly of α -Se monolayers. Experimentally, only an α -Se bilayer has been synthesized successfully [27]. Numerical results for the cohesive energies and structural parameters of the Se allotropes shown here are summarized in Table I.

E_{coh} values of all 1D and quasi-2D Se allotropes have been calculated using total energy differences with respect to isolated Se atoms. The dynamical stability of the four quasi-2D Se allotropes discussed in this work has been confirmed by the phonon spectra displayed in Fig. 2. As an independent proof

TABLE I. Results of our DFT-PBE-D2 calculations for the optimum bond angle γ , the dihedral angle ψ , and the cohesive energy E_{coh} of the various Se allotropes investigated in our study.

	α -helix	b -chain	c -helix	d -chain	α -Se	δ -Se	τ -Se	η -Se
γ (degrees)	103	104; 107	113	103; 106	101; 104	103; 105	109	106; 105
ψ (degrees)	100	101; 91	64	79; 100	99; 103	98; 103	43; 78	77; 99
E_{coh} (eV/atom)	3.359	3.376	3.361	3.373	3.476	3.488	3.462	3.498

of dynamic stability, we have performed finite-temperature molecular dynamics (MD) simulations of these systems. We have found the quasi-2D α -Se, δ -Se, and η -Se structures to be stable at $T = 300$ K, but τ -Se to be stable only at the lower temperature of $T = 200$ K. Additional information about the MD simulations is presented in Section D of the Appendix.

The reason why we call these allotropes “quasi-2D” and not “2D” or “1D” is that the interchain interaction within the layer is much smaller than that of covalent bonds, but still stronger than the interlayer “vdW” interaction. Our DFT calculations based on the PBE-D2 functional show that in comparison to isolated 1D structures, the quasi-2D allotropes gain $\Delta E = 117$ meV/atom in α -Se, $\Delta E = 112$ meV/atom in δ -Se, $\Delta E = 101$ meV/atom in τ -Se, and $\Delta E = 125$ meV/atom in η -Se. This interaction also changes the bond angles γ and the dihedral angles ψ in each 1D subsystem of these quasi-2D allotropes. Typical changes are $\Delta\gamma, \Delta\psi \lesssim 2^\circ$ in α -Se, $\Delta\gamma \lesssim 5^\circ$ and $\Delta\psi \lesssim 8^\circ$ in δ -Se, $\Delta\gamma \lesssim 5^\circ$ and $\Delta\psi \lesssim 21^\circ$ in τ -Se, and $\Delta\gamma \lesssim 2^\circ$ and $\Delta\psi \lesssim 3^\circ$ in η -Se.

Assembly of isolated 1D structures to layers also leads to a charge redistribution that may cause polarization changes in the system. Bader charges of individual Se atoms, which

were all the same in isolated chains, change by $\Delta Q \approx 0.05e$ in α -Se, $\Delta Q \approx 0.02e$ in τ -Se, $\Delta Q \approx 0.04e$ in δ -Se, and $\Delta Q \approx 0.05e$ in η -Se. Such charge transfers are a signature of forming local electric dipoles. Judging from Figs. 3(a)–3(d), we can clearly see a depletion of the electron density in the space in-between the chains and charge redistribution among the inequivalent Se atoms. A similar change in the charge density has been reported in bilayer phosphorene [28], where $\approx 0.075e$ per P atom have been redistributed in comparison to a superposition to monolayer charge densities, which would not be expected in a purely vdW-bonded system.

Ferroelectricity in well-studied 3D systems such as BaTiO₃ [9,10] and PbTiO₃ [11,12] is associated with the relative displacement of sublattices, which is characterized by the position of a representative atom within the unit cell. In the most symmetric, but least stable geometry, which we may call B_S and which places this atom in the center of the unit cell, makes the system a paraelectric (PE) with no local dipole moments. Displacing this atom from the unstable B_S state along a favorite direction to the most stable geometry A results in an energy gain and formation of local electric dipoles causing FE behavior. Displacing the atom in the opposite direction to an equivalent geometry A' only flips the direction of the polarization by 180° .

The situation in our study is much more complex. We deal not only with one atom within a unit cell, but with many atoms in a chain segment that has an axial rotation degree of freedom. Also the calculation of the polarization using the Berry phase approach is more complex than in the above 3D systems and is presented in detail in Appendix A.

Our calculations indicate that α -Se and δ -Se are ferroelectrics with the polarization values $P = 2.53$ pC/cm in α -Se and $P = 2.96$ pC/cm in δ -Se. These values are comparable

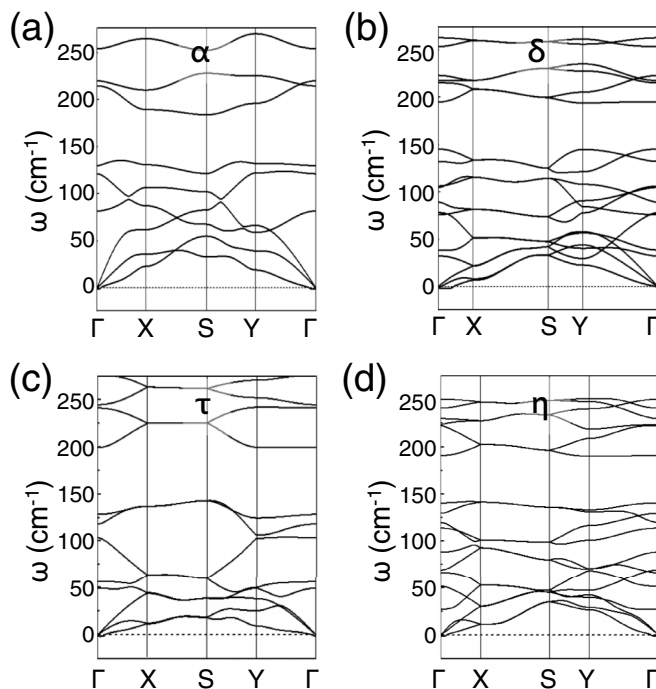


FIG. 2. Phonon spectra of quasi-2D (a) α -Se, (b) δ -Se, (c) τ -Se, and (d) η -Se.

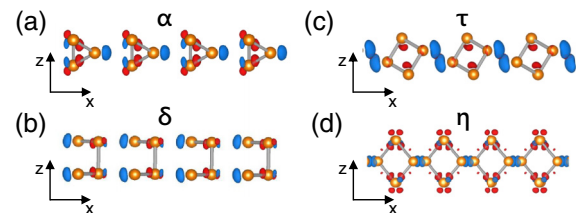


FIG. 3. Charge redistribution caused by connecting isolated 1D Se chains to quasi-2D (a) α -Se, (b) δ -Se, (c) η -Se, and (d) τ -Se assemblies. Calling the optimum geometry of the quasi-2D states the A structure, we display the difference charge density $\Delta\rho = \rho(A) - \rho(\text{isolated-1D})$ as isosurfaces bounding regions of electron excess at $+2.5 \times 10^{-3} \text{ e}/\text{\AA}^3$, shown in red, and electron deficiency at $-2.5 \times 10^{-3} \text{ e}/\text{\AA}^3$, shown in blue.

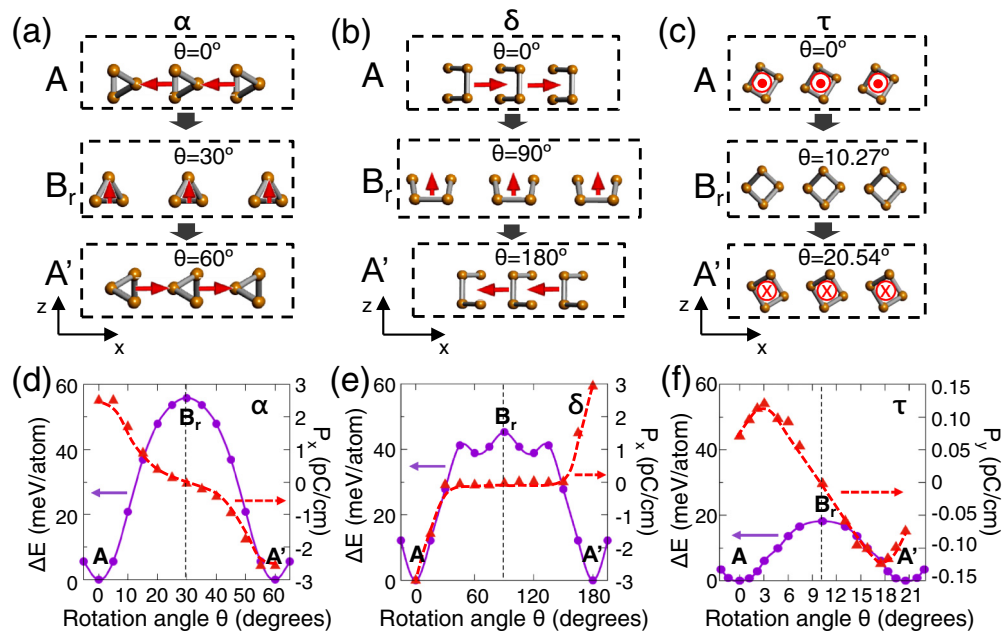


FIG. 4. Axial chain rotation process about the angle θ in quasi-2D Se allotropes. Shown is the transition from the initial state A , across the rotational barrier state B_r , to the closest energetically degenerate state A' with the opposite polarization direction. [(a)–(c)] Morphology and polarization and [(d)–(f)] energy changes in α , δ , and τ allotropes of Se. The electric dipole moment is shown by the red arrow, with \odot representing the out-of-plane and \otimes the into-the-plane directions.

to values observed in typical 2D monochalcogenide ferroelectrics of group IV elements [29–31], such as GeS, SnS, or SnSe. In τ -Se, a net electric polarization of $P_\tau = 0.07$ pC/cm points along the \bar{a}_1 direction. In the following, we will not discuss η -Se with an AFE behavior and a vanishing net polarization, but will focus on α -Se, δ -Se, and τ -Se with a nonvanishing polarization.

Within the chalcogen group, tellurium (Te) should be similar to Se not only in its chemical behavior, but also in its electronic properties. As could be expected, results published for β -Te indicate that this 2D allotrope displays about half the polarization found in Se, since systems containing this heavier element are more metallic [32].

Even though the interchain interaction in the 2D systems discussed here is stronger than a pure vdW interaction, it is weaker than a covalent interaction, thus allowing this rotational degree of freedom to be activated at moderate energy cost. We may thus expect gradual changes in the magnitude and direction of the polarization when activating the axial rotation degree of freedom.

B. Tunability of the polarization by chain rotation

Unlike in uniform, traditional 2D materials, where all atoms are connected by strong chemical bonds of typically $\gtrsim 1$ eV/atom, the quasi-2D allotropes of Se we consider here consist of 1D chains bonded by a weaker interchain interaction of around 0.1 eV/atom. This weaker interaction does not restrict the rotation of individual constituent chains. Whereas in-plane strain, applied to a general 2D system, changes the atomic structure, it usually maintains the symmetry. Rotation of the individual chains by a nonzero angle θ , however, does

modify the symmetry of the system. As a result, the polarization of the system, which is related to symmetry, will also be modified.

As also implied in Figs. 4(a)–4(c), the initial ground state structure A with $\theta = 0^\circ$ is equivalent to the A' structure with the same symmetry for $\theta = 60^\circ$ in α -Se, $\theta = 180^\circ$ in δ -Se, and $\theta = 20.54^\circ$ in τ -Se. The energetically degenerate structures A and A' are related to each other by a 180° rotation of the system about an axis normal to the plane. Thus the polarization direction is reversed between A and A' .

Rotation of individual chains within the quasi-2D layer is an energetically activated process, with the barriers related to the interchain interaction. For simpler systems, the transition path is usually determined using the nudged elastic band (NEB) approach. Considering the number of atoms per unit cell, each with 3 degrees of freedom, and the possibility of Bravais lattice vector changes, optimizations would have to be performed in a roughly 20-dimensional configuration space, well beyond the scope of NEB. To be tractable, we make specific assumptions about the path in configuration space in an approach dubbed “poor-man’s NEB” that has been introduced previously [24]. For each rotation angle, kept as a constraint, we optimized the interchain distance and then the atomic positions. This approach may overshoot the value of the activation barrier at B_r , between the ground-state structures A and A' , but is still useful to characterize a likely path in configuration space involving chain rotations that leads to changes in polarization. The values of the activation barriers between equivalent configurations, determined in this way, are 60 meV/atom for α -Se, 50 meV/atom for δ -Se, and 20 meV/atom for τ -Se, as shown in Figs. 4(d)–4(f). We validated our approach by calculating the phonon spectra at

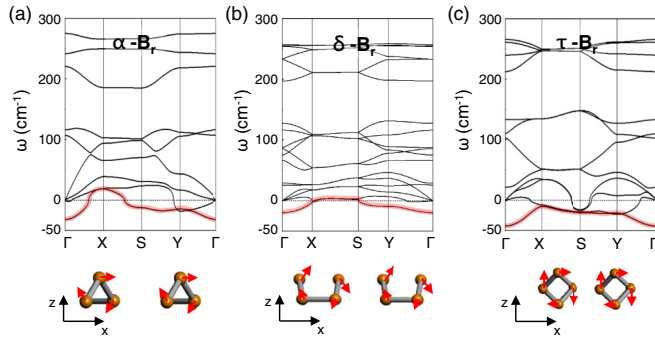


FIG. 5. Phonon spectra of the transition state structure B_r , which is unstable with respect to the rotation of constituent chains in (a) α -Se, (b) δ -Se, and (c) τ -Se. The lowest branch of the phonon spectra with imaginary frequency is highlighted by the red line. Corresponding modes, initiating structural change, are indicated by the red arrows in the bottom panels.

the unstable transition structure B_r and present our results in Fig. 5. As expected, we observe a soft mode with an imaginary frequency that is characterized at Γ by the rotation of the constituent 1D chains towards the more stable A or A' structures in α - B_r , δ - B_r and τ - B_r .

During the chain rotation from state A to A' , significant changes occur in the electronic structure and especially the polarization. Our results indicate that both out-of-plane and in-plane polarization components are changing, with the polarization direction depicted in Figs. 4(a)–4(c) and the value of the in-plane component of the polarization shown in Figs. 4(d)–4(f).

An independent Bader charge calculation indicates that polarization changes are caused by charge reorganization during the rotation of individual chains. We have found that rotation of a -chains in α -Se changes Bader charges on individual atoms by $\Delta Q \approx 0.01e$. According to Fig. 4(a), changing the rotation angle from geometry A with $\theta = 0^\circ$ to geometry A' with $\theta = 60^\circ$ flips the direction of the in-plane polarization. At the transition state B_r with $\theta = 30^\circ$, the polarization direction changes to out-of-plane with a value of $P = 0.02$ pC/cm. A similar change in polarization occurs in δ -Se according to Fig. 4(b) during a rotation by $\Delta\theta = 180^\circ$. For this system, $\Delta Q \approx 0.03e$, and the transition state B_r at $\theta = 90^\circ$ acquires an out-of-plane polarization of $P = 0.017$ pC/cm. According to Fig. 4(c), the behavior of τ -Se during the rotation of the constituent c -helices is quite different. Unlike in the previous cases, the in-plane polarization direction is along and not normal to the chains, but still flips its direction during a rotation by $\Delta\theta = 20.54^\circ$. At the activation barrier state B_r with $\theta = 10.27^\circ$, the system turns into a highly symmetric paraelectric with a vanishing polarization.

C. Tunability of the band structure by chain rotation

Not only the net polarization, but also the band structure of the system is affected by the chain rotation. Results of our DFT-PBE calculations, presented in Figs. 6(a)–6(c), suggest that all Se allotropes discussed here are semiconductors with fundamental band gaps of 1.70 eV in α -Se, 1.99 eV in δ -Se,

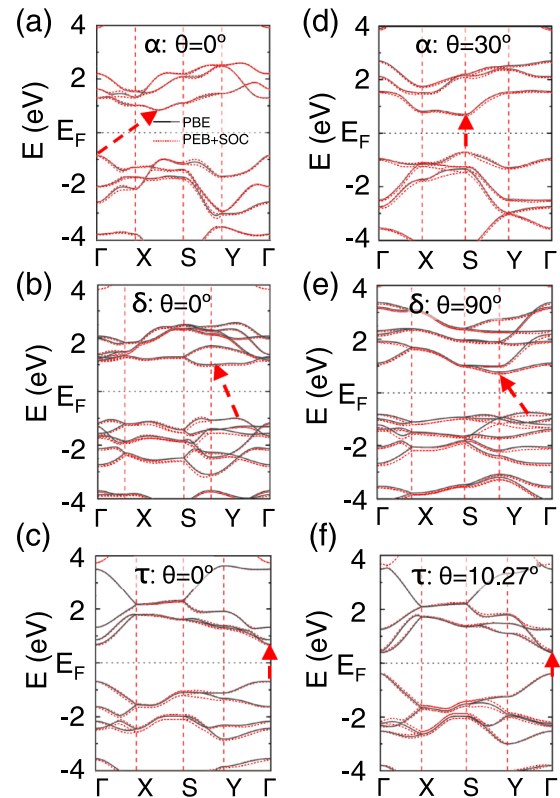


FIG. 6. Effect of the axial rotation angle θ of the constituent 1D structures on the electronic band structure $E(\mathbf{k})$ in quasi-2D Se allotropes. $E(\mathbf{k})$ in α -Se is shown for (a) $\theta = 0^\circ$ and (d) $\theta = 30^\circ$, in δ -Se for (b) $\theta = 0^\circ$ and (e) $\theta = 90^\circ$, in τ -Se for (c) $\theta = 0^\circ$ and (f) $\theta = 10.27^\circ$. PBE-D2 results without spin-orbit coupling (SOC) are presented by the solid black lines and those with SOC by the dashed red lines.

and 1.38 eV in τ -Se. We have repeated these calculations by specifically considering the effect of spin-orbit coupling (SOC). Since the results with and without SOC, presented in Fig. 6, are very similar, we conclude that the role of SOC is not significant in our systems. Whereas the band gap values are typically underestimated in DFT calculations, the band dispersion is expected to be correct. Even though the systems are strongly anisotropic, the band dispersion along the Γ - X direction along the quasi-1D chains is not significantly smaller than along the Γ - Y direction normal to it. We expect α -Se and δ -Se to be indirect-gap semiconductors, whereas τ -Se should have a direct band gap at the Γ point. In α -Se, rotating the individual a -helices by 30° reduces the fundamental band gap to 1.40 eV and turns it into a direct gap near the S -point, as seen in Fig. 6(d). As seen in Fig. 6(e), a 90° rotation of the b -chains in δ -Se causes a reduction of the band gap to 1.55 eV, but keeps the gap indirect. According to Fig. 6(f), the band gap in τ -Se remains indirect, but is reduced to 0.80 eV as the c -helices rotate by 10.27° .

D. Effect of in-plane strain on the polarization of quasi-2D Se allotropes

We also study the effect of in-plane uniaxial strain on the polarization. To do so, we strain the lattice uniformly along the

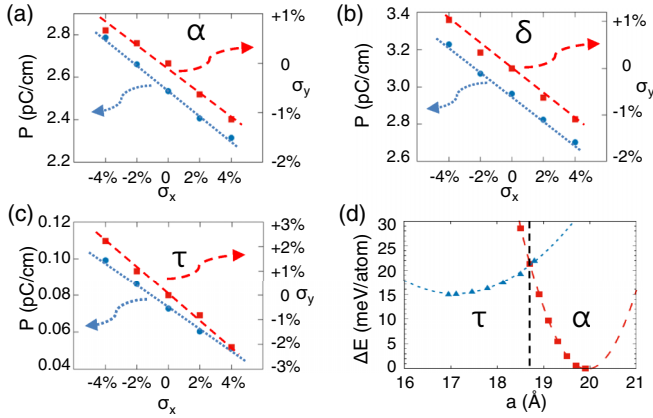


FIG. 7. Net polarization P and deformation σ_y along the \bar{a}_2 direction as a function of uniaxial strain σ_x along the \bar{a}_1 direction in quasi-2D (a) α -Se (b) δ -Se, and (c) τ -Se. The effect of σ_x on P is shown by the blue dotted lines, and corresponding changes in σ_y are shown by the red dashed line. (d) Energy change ΔE caused by changing the lattice constant a in τ -Se and α -Se along the \bar{a}_1 direction. Results for supercells of α -Se, with $a = 4a_1(\alpha - \text{Se})$, are shown by the red dashed line. Results for supercells of τ -Se, with $a = 3a_1(\tau - \text{Se})$, are shown by the blue dotted line.

\bar{a}_1 direction, which is aligned with the axes of the constituent chains in α -Se, δ -Se, and τ -Se. To reproduce the realistic response of a system subject to this strain, we allow the a_2 lattice constant to relax for each value of a_1 . As the quasi-2D structures are stretched along the \bar{a}_1 direction, they shrink linearly along the \bar{a}_2 direction, indicating a positive Poisson ratio.

For α -Se shown in Fig. 7(a) and δ -Se in Fig. 7(b), the change in the lattice constant a_2 is about one fourth of the change in the lattice constant a_1 along the chain axis. The resulting Poisson ratios are $\nu \approx 0.22$ for α -Se and $\nu \approx 0.27$ for δ -Se. According to Fig. 7(c), the Poisson ratio of τ -Se, $\nu \approx 0.54$, is about twice that of δ -Se.

The net polarization as a function of strain is also shown in Figs. 7(a)–7(c). These results indicate a linear increase in the polarization as the structure is compressed along the chain axis. For the uniaxial strain value $\sigma_x = -4\%$, we observe an increase in the polarization by 9.8% in α -Se, 9.1% in δ -Se, and by 37.5% in τ -Se.

As can be inferred from Figs. 1(a) and 1(c), the a -helix component of α -Se and the c -helix component of τ -Se are topologically related. They can be transformed from one to another by a twisting/untwisting process, in which the bond angles and the dihedral angles change. We should note that for supercells containing the same number of atoms, the lattice constant along the chain direction is $a = 4a_1$ for α -Se and $a = 3a_1$ for τ -Se. The energy change ΔE as a function of the supercell length in these two allotropes is shown in Fig. 7(d). We set the optimum structure of the more stable α -Se allotrope as the energy reference, with the optimum τ -Se structure being less stable by only 15 meV/atom. At the supercell lattice constant $a = 18.72 \text{ \AA}$, the energy of stretched τ -Se equals that of compressed α -Se, indicating the possibility of a strain-induced phase transformation at this point.

E. Effect of in-plane strain on the band structure of quasi-2D Se allotropes

We also study the effect of in-plane uniaxial strain on the band structure of α -Se, δ -Se and τ -Se. Our results, presented in Fig. 8, indicate that the three allotropes keep their semi-conducting character when the quasi-1D structures are axially compressed or stretched, with strain values σ_x ranging from -4% to $+4\%$. Similar to our results for unstrained systems in Fig. 6, α -Se and δ -Se remain indirect-gap semiconductors, whereas τ -Se has a direct band gap at the Γ point independent of strain. We find that the fundamental band gap widens under compression and shrinks in stretched systems. In particular, under $\sigma_x = -4\%$ compression, E_g increases by 14% in α -Se, 3.5% in δ -Se and 3.6% in τ -Se. Under $\sigma_x = +4\%$ stretch, E_g decreases by 20% in α -Se, 5.4% in δ -Se and 2.5% in τ -Se. This behavior does not follow the naive picture for 1D systems that stretching elongates bonds, thus reducing hopping and the bandwidth, leading to wider band gaps. In the quasi-2D systems that we study, stretching the chains reduces the interchain distance and thus increases the interchain interaction. Since the band dispersion along and normal to the chain direction is comparable, the naive picture of 1D systems no longer applies, resulting in dispersion changes seen in Fig. 8.

IV. DISCUSSION

We studied the possibility to tune the electric polarization of four quasi-2D allotropes of Se. Besides α -Se, the naturally occurring phase consisting of a -helices, we also studied δ -Se, η -Se and τ -Se, which differ only in their dihedral angles and should be similarly stable. The transformation of the a -helix to a b -chain, the constituent of δ -Se, has been discussed earlier [24]. A change of the dihedral angle leads to the d -chain of η -Se, and untwisting the a -helix leads to the c -helix of τ -Se. Interaction of these 1D structures should, as in the case of α -Se, lead to the formation of corresponding quasi-2D structures. Since the unit cells of these four allotropes are very different, selecting a suitable substrate with a matching lattice constant should cause preferential epitaxial growth of a given allotrope. Charge redistribution due to the interchain interaction causes a net electric polarization in many of these quasi-2D allotropes.

Our calculations of the polarization behavior in these unusual systems are performed using a well-established approach [32], where we first identify a related, highly symmetric paraelectric structure with no local dipoles, which we call B_S . For the sake of completeness, we provide specific details about the construction of the B_S state in Appendix A. The nature of the polarization behavior is then deduced by comparing the charge distribution in a given system to that in the B_S state.

Changes of the electric polarization in ferroelectrics are caused by relative displacement of sublattices. In most common ferroelectrics including BaTiO_3 , the interaction among atoms forming such sublattices is indirect, effectuated by strong covalent or ionic bonds to atomic neighbors in other sublattices. In absence of a hierarchy of weaker and stronger interactions in the system, a selective mechanical displacement of a sublattice appears impossible.

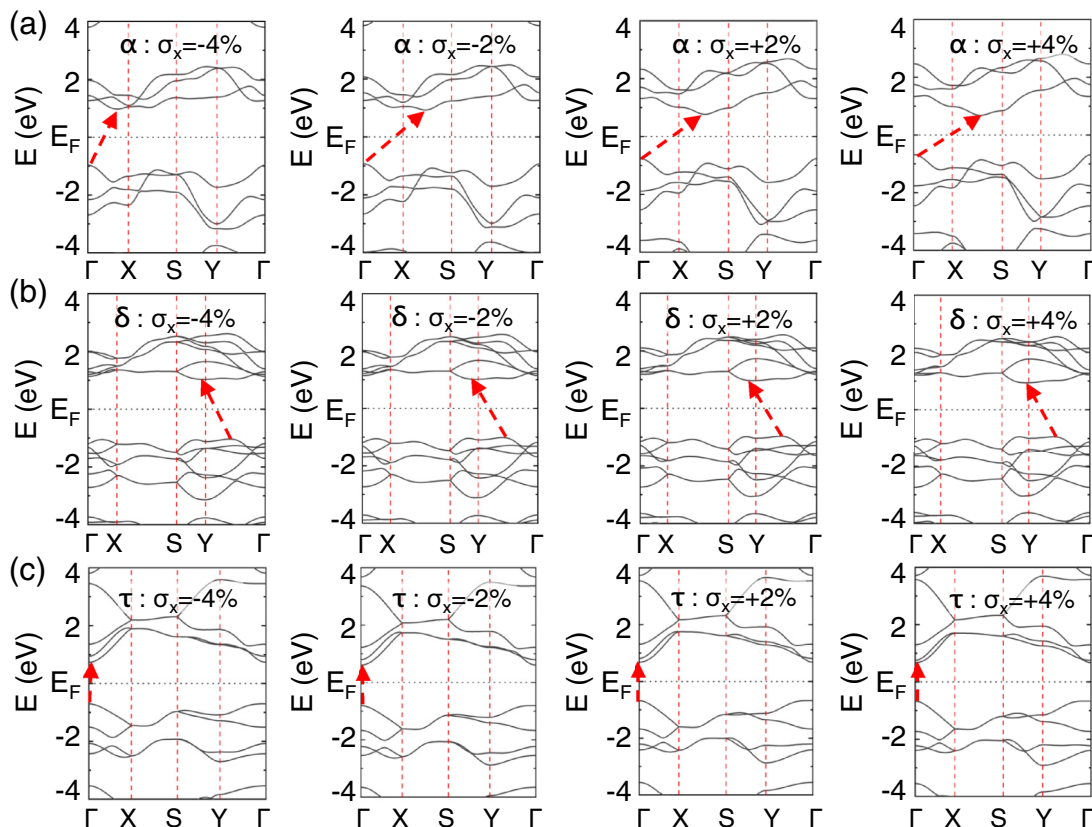


FIG. 8. Effect of the uniaxial strain σ_x along the chain direction on the electronic band structure $E(k)$ in (a) α -Se (b) δ -Se, and (c) τ -Se. Lowest-energy transitions across the fundamental band gap are indicated by the red dashed lines and arrows.

The situation is very different in quasi-2D Se allotropes discussed here, which consist of covalently bonded 1D constituents that form sublattices. The weaker interaction between the 1D systems provides one additional degree of freedom, namely, the axial rotation. This rotation, as we have shown, may change not only the magnitude, but also the direction of the polarization from in-plane to out-of-plane. We can imagine two scenarios to effectuate such a rotation.

One of these scenarios uses nanosized combs that have been synthesized recently [33,34]. We can imagine a comb structure pressing from top onto a quasi-2D Se structure adsorbed on a substrate. Inserting the “teeth” of the comb in-between the chains and moving them along the chain direction should result in a torque that would rotate each chain. The other scenario is to place the quasi-2D system within a planar interface in-between two solid blocks in a sandwich configuration. Applying in-plane shear while pressing the blocks together should cause the quasi-1D components to rotate like tree logs on a wagon. In both cases, we estimate that a torque $>10^{-20}$ N m per unit cell should be required to initiate the rotation of chains. Strain transfer to the quasi-2D allotropes will be most efficient when using solid blocks with a high Young’s modulus such as polydimethylsiloxane or polyvinyl alcohol [35,36].

We also imagine two scenarios to flip the direction of the polarization in our quasi-2D Se allotropes. Both scenarios involve atomic motion across a barrier in an energetically activated process. In the first scenario, which involves a higher activation energy and is discussed in more detail in

Appendix C, atoms in a rigid unit cell are displaced in opposite directions from the initial state A, across a highly symmetric transition state B_S , to the final state A' with the same energy as A. This process is shown in Figs. 11(a)–11(c). Since the bond lengths and bond angles change significantly during this process, the energy cost is rather high, amounting to 80.1 meV/atom in α -Se, 106.4 meV/atom in δ -Se, and 40.3 meV/atom in τ -Se according to Figs. 11(d)–11(f).

The second scenario involves a special rotation of the constituent 1D structures in the quasi-2D Se system, as illustrated in Fig. 4. In comparison to the first scenario, the energy investment here is lowered to about 69.7% for α -Se, 42.5% for δ -Se, and 45.1% for τ -Se of its initial value. Thus we may expect that applying an external electric field may cause an axial rotation of rigid 1D structures rather than atomic displacement within a rigid unit cell. Clearly, lowering the interchain interaction should lower the energy cost, allowing the chains to rotate more easily. On the other hand, the interchain interaction must be significant enough to cause charge redistribution and lead to polarization. We believe that the quasi-2D Se allotropes discussed here bring a good balance of both effects, providing the possibility to tune the polarization by allowing for structural changes at a very moderate energy cost.

The high flexibility of 1D Se chains in terms of bond length, bond angle and dihedral angle suggests that many more structures beyond the four allotropes discussed here may be realized, resulting in other quasi-2D structures with very different electronic properties.

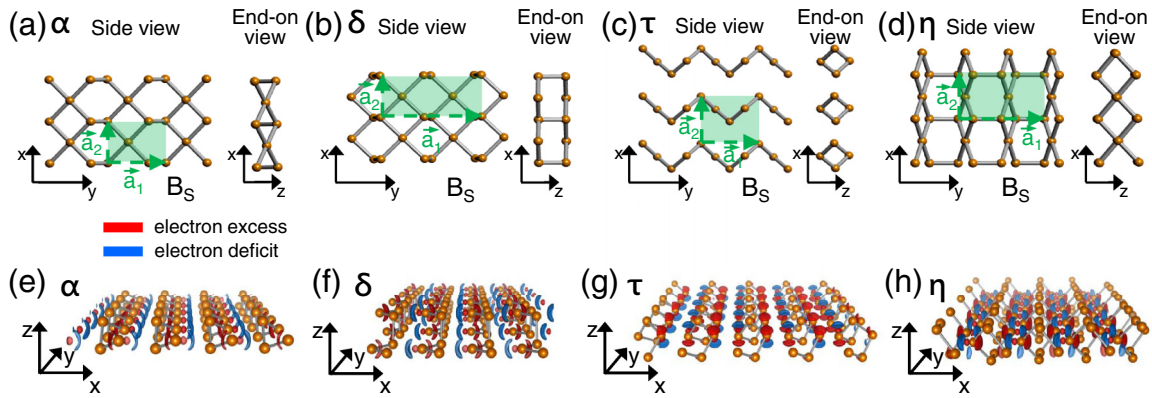


FIG. 9. Highly symmetric paraelectric phase B_S of quasi-2D allotropes of Se placed in the x - y plane. The structure of (a) α -Se, (b) δ -Se, (c) τ -Se, and (d) η -Se is shown in the side and the end-on view. The unit cells are highlighted by the transparent green areas. (e)–(h) display the charge redistribution $\Delta\rho = \rho(A) - \rho(B_S)$ between the polarized phase of α -Se, δ -Se, τ -Se, and η -Se and their highly symmetric PE phase with no local dipoles, which we call the B_S state in the text. Isosurfaces of $\Delta\rho$ are represented by bounding regions of electron excess at $+7 \times 10^{-2} \text{ e}/\text{\AA}^3$ (red) and electron deficiency at $-7 \times 10^{-2} \text{ e}/\text{\AA}^3$ (blue). The electric polarization is thus pointed from the red to the blue region.

V. SUMMARY AND CONCLUSIONS

In summary, we have performed *ab initio* DFT calculations to study the polarization and band structure of four quasi-2D allotropes of Se, which we called α -Se, δ -Se, η -Se, and τ -Se. These allotropes are formed from their 1D constituents, which we call the a -helix, b -chain, c -helix, and d -chain, and which possess a rotational degree of freedom about their axis. The interchain interaction is not strong enough to suppress the rotation of these chains, but still causes a charge redi-

tribution within the quasi-2D structures that results in a net polarization. α -Se and δ -Se display an FE behavior with an in-plane polarization, directed normal to the 1D chains. An in-plane polarization also occurs in η -Se, which displays an AFE behavior. τ -Se behaves as a noncollinear ferrielectric, with FE polarization along the chain axis and AFE polarization in the out-of-plane direction. Rotating each constituent 1D chain in these quasi-2D Se allotropes changes the atomic symmetry and also the electronic structure. In the α and δ

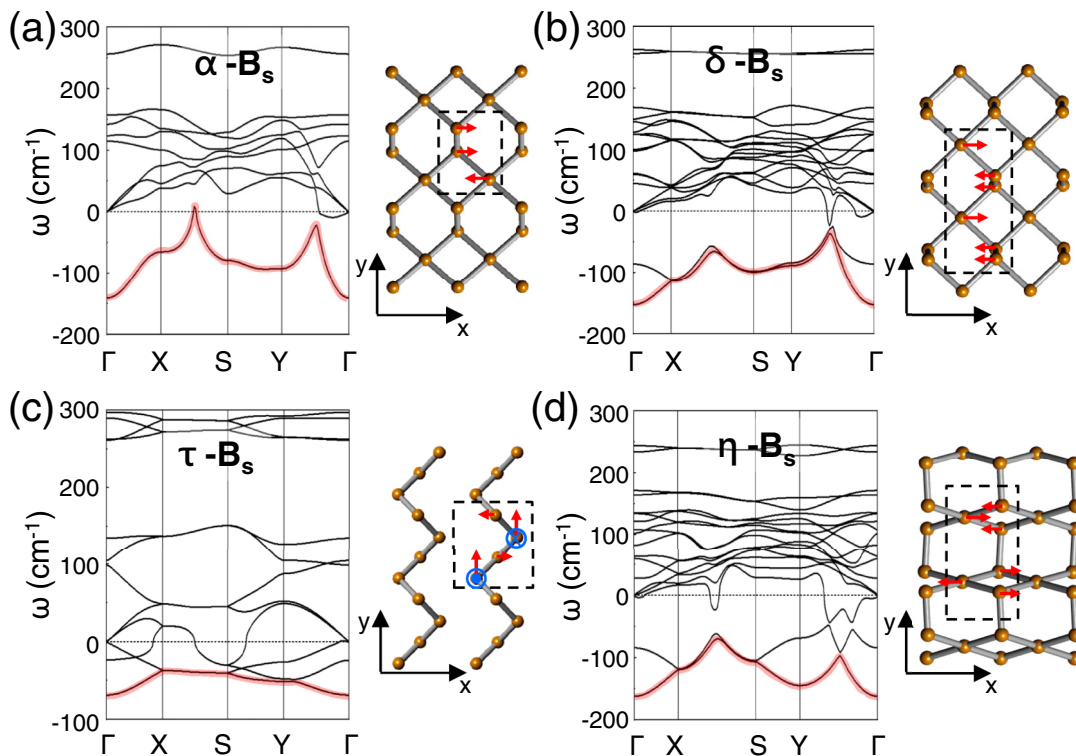


FIG. 10. Phonon spectra of the paraelectric phase B_s of (a) α -Se, (b) δ -Se, (c) τ -Se, and (d) η -Se. The vibration mode of the lowest branch of the phonon spectra which is highlighted by red line is represented by the red arrow in the right panel. \odot and \otimes in (c) representing the out-of-plane and the into-the-plane displacements of Se atoms.

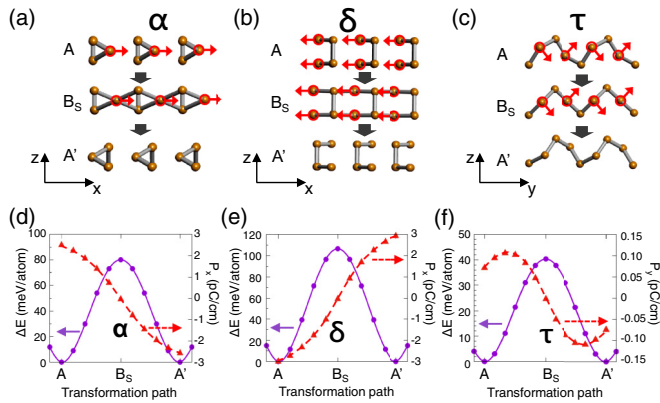


FIG. 11. Structural changes causing a flip of the polarization direction in quasi-2D allotropes of Se. Atomic displacement, indicated by the red arrows, starts from the initial state A , crosses the paraelectric state B_S , and is completed in the final state A' of (a) α -Se, (b) δ -Se, and (c) τ -Se. Corresponding energy changes ΔE in (d) α -Se, (e) δ -Se, and (f) τ -Se.

allotropes, chain rotation changes the polarization direction from in-plane to out-of-plane. At specific rotation angles, τ -Se distorts to a highly symmetric structure and its FiE polarization disappears. Along with changes in polarization, caused by chain rotation, come changes in the electronic band structure of these semiconducting allotropes including a modification of the fundamental band gap, which may change from an indirect to a direct gap in δ -Se. In-plane strain along the axial direction of the 1D structures only modifies the magnitude of the polarization.

ACKNOWLEDGMENTS

We appreciate valuable discussions with Bei Zhao and Wei Liu about the rotation strategy. D.L. acknowledges financial support by the Natural Science Foundation of the Jiangsu Province Grant No. BK20210198. R.W. and S.D. acknowledge financial support by the National Natural Science Foundation of China (NNSFC) Grant No. 11834002. S.S. and J.G. acknowledge financial support by NNSFC Grant No. 61704110. Computational resources for most calculations have been provided by the Michigan State University High Performance Computing Center.

APPENDIX

A. Polarization calculation using the Berry phase approach

Polarization studies of a given allotrope using the Berry phase approach begin with the construction of a highly symmetric PE counterpart of this allotrope with no local electric dipoles. Specifics of the construction process are outlined in Appendix B. For the allotropes in this study, we display the morphology of the PE state, characterized by the symbol B_S , in Fig. 9, and determine their charge distribution. Structural optimization of the B_S state in these allotropes causes a reduction of the space group symmetry from $P2m$ to $P2$ in α -Se, from $Pmma$ to $Pma2$ in δ -Se, and from $Pmma$ to $P2_1$ in η -Se.

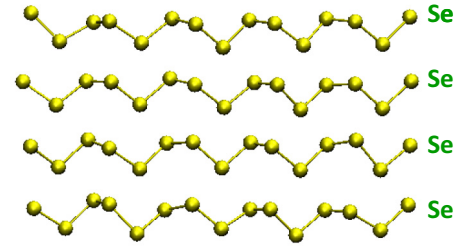


FIG. 12. Representative snapshot of a 2 ps long MD simulation of α -Se at $T = 300$ K. The full video is presented in Ref. [37].

This essentially translates to loss of mirror symmetry with respect to a plane normal to the interchain direction.

Comparing the charge difference between these quasi-2D allotropes and their corresponding B_S states, we observe a parallel electrical polarization along the \bar{a}_2 direction of α -Se and δ -Se indicating FE behavior, shown in Figs. 9(e) and 9(f). And an antiparallel electrical polarization along the \bar{a}_2 direction of η -Se indicating an AFE behavior, shown in Fig. 9(h). A special behavior occurs in the unit cell of τ -Se. In comparison to the B_S structure, two positively charged atoms both move in the same direction along \bar{a}_1 , but in opposite directions normal to the plane. The space group symmetry $P222_1$ reduces to $P2_1$ in τ -Se, as the rotation symmetry about \bar{a}_2 and about the direction normal to the layer in the B_S structure is lost, with only the rotation symmetry about \bar{a}_1 remaining. As a result, τ -Se displays a noncollinear polarization behavior, indicated in Fig. 9(g). We use the term “FiE,” which is defined for the similar noncollinear polarization in a δ -GeS monolayer [31], to describe the polarization behavior in τ -Se. The polarization of the quasi-2D Se allotropes discussed here is shown by the red arrows in Figs. 1(f)–1(i).

B. Construction and characterization of the PE state in quasi-2D Se allotropes

We use a traditional approach to construct the highly symmetric paraelectric state called B_S . We start from the initial structure A and identify the polarization direction. We reflect A about a mirror plane that is perpendicular to the polarization direction to arrive at A' . Since A and A' are mirror symmetric,

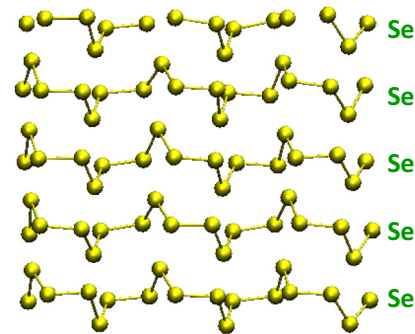


FIG. 13. Representative snapshot of a 2 ps long MD simulation of η -Se at $T = 300$ K. The full video is presented in the SM [37].

the polarization of A' is opposite to that of A . A state mid-way between A and A' has zero polarization and is identified as the paraelectric reference state B_S . As can be seen in Fig. 9, such paraelectric structures have a higher symmetry in comparison to the initial state A shown in Fig. 1.

We calculate the phonon spectra of these paraelectric structures B_S and show the results in Fig. 10. The phonon mode associated with the largest imaginary frequency at the Γ point indicates a decay to more stable structures A and A' .

C. Flipping the polarization by atom displacement

One possible way to flip the polarization direction in the quasi-2D allotropes by 180° is to displace specific atoms within the unit cell in a particular way. Let us focus on α -Se, δ -Se, and τ -Se with a nonzero polarization. Starting from the initial state A , we displace specific atoms along the direction indicated by the red arrows in Fig. 11. The displacement continues across the barrier state B_S shown in Fig. 9 and completes at the state A' . The stability of A and A' is the same, but the polarization is opposite. The atomic displacement process causing a flip of the polarization direction is shown in Fig. 11(a) for α -Se, Fig. 11(b) for δ -Se, and Fig. 11(c) for τ -Se. The energy barrier in this process is $\Delta E \approx 80.08$ meV/atom for α -Se, $\Delta E \approx 106.41$ meV/atom for δ -Se, and $\Delta E \approx 40.3$ meV/atom for τ -Se, as seen in Figs. 11(d)–11(f). The gradual change of polarization caused by atom displacement is shown by the red dashed lines in Figs. 11(d)–11(f). Starting from the most stable state A , the polarization first decreases to zero at the paraelectric reference state B_S , and then increases to the initial value with opposite direction at the final state A' .

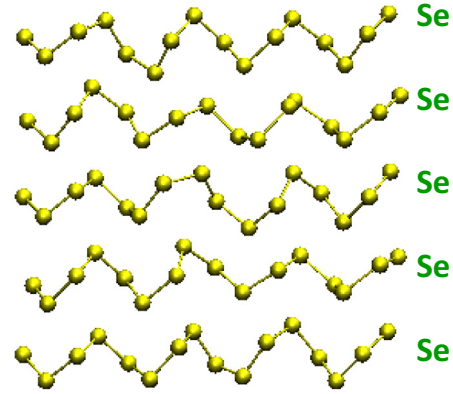


FIG. 14. Representative snapshot of a 2 ps long MD simulation of τ -Se at $T = 200$ K. The full video is presented in the SM [37].

D. Finite-temperature MD simulations of quasi-2D Se structures

We have performed canonical MD simulations at finite temperature as an independent proof of the thermodynamic stability of the quasi-2D α -Se, η -Se, and τ -Se structures described in the main text. Results are presented as videos in Ref. [37]. Snapshots of 2 ps long runs at $T = 300$ K are shown in Fig. 12 for α -Se and in Fig. 13 for η -Se. Results of a 2 ps run for δ -Se at $T = 300$ K were published earlier [24]. As can be inferred from Figs. 4 and 11, the energy barrier in τ -Se is much smaller than in α -Se and δ -Se. Thus we have also found τ -Se to become unstable at 300 K. Therefore we have used a lower temperature $T = 200$ K for the 2 ps run of τ -Se and present a representative snapshot in Fig. 14.

- [1] E. Schrödinger, Studien über Kinetik der Dielektrika, den Schmelzpunkt, Pyro- und Piezoelektrizität, Sitzungsberichte der Kaiserl. Akademie der Wissenschaften in Wien. Mathem.-naturw. Klasse **121**, 1 (1912).
- [2] Minutes of the Washington Meeting, April 23 and 24, 1920, *Phys. Rev.* **15**, 505 (1920).
- [3] J. Valasek, Piezo-electric and allied phenomena in Rochelle salt, *Phys. Rev.* **17**, 475 (1921).
- [4] Z. Guan, H. Hu, X. Shen, P. Xiang, N. Zhong, J. Chu, and C. Duan, Recent progress in two-dimensional ferroelectric materials, *Adv. Electron. Mater.* **6**, 1900818 (2020).
- [5] W. Ding, J. Zhu, Z. Wang, Y. Gao, D. Xiao, Y. Gu, Z. Zhang, and W. Zhu, Prediction of intrinsic two-dimensional ferroelectrics in In_2Se_3 and other $\text{III}_2\text{-VI}_3$ van der Waals materials, *Nat. Commun.* **8**, 14956 (2017).
- [6] F. Liu, L. You, K. L. Seyler, X. Li, P. Yu, J. Lin, X. Wang, J. Zhou, H. Wang, H. He, S. T. Pantelides, W. Zhou, P. Sharma, X. Xu, P. M. Ajayan, J. Wang, and Z. Liu, Room-temperature ferroelectricity in CuInP_2S_6 ultrathin flakes, *Nat. Commun.* **7**, 12357 (2016).
- [7] J. Xiao, H. Zhu, Y. Wang, W. Feng, Y. Hu, A. Dasgupta, Y. Han, Y. Wang, D. A. Muller, L. W. Martin, P. A. Hu, and X. Zhang, Intrinsic Two-Dimensional Ferroelectricity with Dipole Locking, *Phys. Rev. Lett.* **120**, 227601 (2018).
- [8] L. Li and M. Wu, Binary compound bilayer and multilayer with vertical polarizations: Two-dimensional ferroelectrics, multiferroics, and nanogenerators, *ACS Nano* **11**, 6382 (2017).
- [9] K. J. Choi, M. Biegalski, Y. L. Li, A. Sharan, J. Schubert, R. Uecker, P. Reiche, Y. B. Chen, X. Q. Pan, V. Gopalan, L.-Q. Chen, D. G. Schlom, and C. B. Eom, Enhancement of ferroelectricity in strained BaTiO_3 thin films, *Science* **306**, 1005 (2004).
- [10] P. Chen, Y. Xu, N. Wang, A. R. Oganov, and W. Duan, Effects of ferroelectric polarization on surface phase diagram: Evolutionary algorithm study of the $\text{BaTiO}_3(001)$ surface, *Phys. Rev. B* **92**, 085432 (2015).
- [11] S. P. Beckman, X. Wang, K. M. Rabe, and D. Vanderbilt, Ideal barriers to polarization reversal and domain-wall motion in strained ferroelectric thin films, *Phys. Rev. B* **79**, 144124 (2009).
- [12] G. Catalan, A. Lubk, A. H. G. Vlooswijk, E. Snoeck, C. Magen, A. Janssens, G. Rispens, G. Rijnders, D. H. A. Blank, and B. Noheda, Flexoelectric rotation of polarization in ferroelectric thin films, *Nat. Mater.* **10**, 963 (2011).
- [13] N. Ding, J. Chen, C. Gui, H. You, X. Yao, and S. Dong, Phase competition and negative piezoelectricity in interlayer-sliding ferroelectric ZrI_2 , *Phys. Rev. Mater.* **5**, 084405 (2021).

- [14] M. Wu and J. Li, Sliding ferroelectricity in 2D van der Waals materials: Related physics and future opportunities, *Proc. Natl. Acad. Sci.* **118**, e2115703118 (2021).
- [15] G. Kresse and J. Furthmüller, Efficient iterative schemes for *ab initio* total-energy calculations using a plane-wave basis set, *Phys. Rev. B* **54**, 11169 (1996).
- [16] G. Kresse and D. Joubert, From ultrasoft pseudopotentials to the projector augmented-wave method, *Phys. Rev. B* **59**, 1758 (1999).
- [17] J. P. Perdew, K. Burke, and M. Ernzerhof, Generalized Gradient Approximation Made Simple, *Phys. Rev. Lett.* **77**, 3865 (1996).
- [18] S. Grimme, Semiempirical GGA-type density functional constructed with a long-range dispersion correction, *J. Comput. Chem.* **27**, 1787 (2006).
- [19] H. J. Monkhorst and J. D. Pack, Special points for Brillouin-zone integrations, *Phys. Rev. B* **13**, 5188 (1976).
- [20] M. R. Hestenes and E. Stiefel, Methods of conjugate gradients for solving linear systems, *J. Res. Natl. Bur. Stand.* **49**, 409 (1952).
- [21] R. D. King-Smith and D. Vanderbilt, Theory of polarization of crystalline solids, *Phys. Rev. B* **47**, 1651 (1993).
- [22] R. Resta, Macroscopic polarization in crystalline dielectrics: the geometric phase approach, *Rev. Mod. Phys.* **66**, 899 (1994).
- [23] T. Fujimori, A. Morelos-Gómez, Z. Zhu, H. Muramatsu, R. Futamura, K. Urita, M. Terrones, T. Hayashi, M. Endo, S. Young Hong, Y. Chul Choi, D. Tománek, and K. Kaneko, Conducting linear chains of sulphur inside carbon nanotubes, *Nat. Commun.* **4**, 2162 (2013).
- [24] D. Liu, X. Lin, and D. Tománek, Microscopic mechanism of the helix-to-layer transformation in elemental group VI solids, *Nano Lett.* **18**, 4908 (2018).
- [25] T. Fujimori, R. dos Santos, T. Hayashi, M. Endo, K. Kaneko, and D. Tománek, Formation and properties of selenium double-helices inside double-wall carbon nanotubes: experiment and theory, *ACS Nano* **7**, 5607 (2013).
- [26] Z. Zhu, X. Cai, S. Yi, J. Chen, Y. Dai, C. Niu, Z. Guo, M. Xie, F. Liu, J.-H. Cho, Y. Jia, and Z. Zhang, Multivalency-Driven Formation of Te-Based Monolayer Materials: A Combined First-Principles and Experimental Study, *Phys. Rev. Lett.* **119**, 106101 (2017).
- [27] P. V. Sarma, R. Nadarajan, R. Kumar, R. M. Patinharayil, N. Biju, S. Narayanan, G. Gao, C. S. Tiwary, M. Thalakulam, R. N. Kini, A. K. Singh, P. M. Ajayan, and M. M. Shaijumon, Growth of highly crystalline ultrathin two-dimensional selenene, *2D Mater.* **9**, 045004 (2022).
- [28] L. Shulenburger, A. D. Baczewski, Z. Zhu, J. Guan, and D. Tománek, The nature of the interlayer interaction in bulk and few-layer phosphorus, *Nano Lett.* **15**, 8170 (2015).
- [29] N. Higashitarumizu, H. Kawamoto, C. Lee, B. Lin, F. Chu, I. Yonemori, T. Nishimura, K. Wakabayashi, W. Chang, and K. Nagashio, Purely in-plane ferroelectricity in monolayer SnS at room temperature, *Nat. Commun.* **11**, 2428 (2020).
- [30] H. Wang and X. Qian, Two-dimensional multiferroics in monolayer group IV monochalcogenides, *2D Mater.* **4**, 015042 (2017).
- [31] S. Song, Y. Zhang, J. Guan, and S. Dong, Noncollinear ferrielectricity and morphotropic phase boundary in monolayer GeS, *Phys. Rev. B* **103**, L140104 (2021).
- [32] Y. Wang, C. Xiao, M. Chen, C. Hua, J. Zou, C. Wu, J. Jiang, S. A. Yang, Y. Lu, and W. Ji, Two-dimensional ferroelectricity and switchable spin-textures in ultra-thin elemental Te multilayers, *Mater. Horiz.* **5**, 521 (2018).
- [33] S. Yang, Y. Wang, L. Wang, G. Zhang, A. Vazinshayan, and A. Duongthipthewa, Growth and characterization of ultra-long ZnO nanocombs, *AIP Adv.* **6**, 065209 (2016).
- [34] S. Lee, A. Sangle, P. Lu, A. Chen, W. Zhang, J. S. Lee, H. Wang, Q. Jia, and J. L. MacManus-Driscoll, Novel electroforming-free nanoscaffold memristor with very high uniformity, tunability, and density, *Adv. Mater.* **26**, 6284 (2014).
- [35] Z. Liu, M. Amani, S. Najmaei, Q. Xu, X. Zou, W. Zhou, T. Yu, C. Qiu, A. G. Birdwell, F. J. Crowne, R. Vajtai, B. I. Yakobson, Z. Xia, M. Dubey, P. M. Ajayan, and J. Lou, Strain and structure heterogeneity in MoS₂ atomic layers grown by chemical vapour deposition, *Nat. Commun.* **5**, 5246 (2014).
- [36] Z. Li, Y. Lv, L. Ren, J. Li, L. Kong, Y. Zeng, Q. Tao, R. Wu, H. Ma, B. Zhao, D. Wang, W. Dang, K. Chen, L. Liao, X. Duan, X. Duan, and Y. Liu, Efficient strain modulation of 2D materials via polymer encapsulation, *Nat. Commun.* **11**, 1151 (2020).
- [37] See Supplemental Material at <http://link.aps.org/supplemental/10.1103/PhysRevMaterials.6.103403> for video files associated with Figs. 12–14.